TÜBİTAK

Turkish Journal of Earth Sciences

http://journals.tubitak.gov.tr/earth/

Research Article

Turkish J Earth Sci
(2013) 22: 632-644
© TÜBİTAK
doi:10.3906/yer-1112-14

Mineralogical and physicochemical properties of talc from Emirdağ, Afyonkarahisar, Turkey

Bahri ERSOY[1], Sedef DİKMEN[2], Ahmet YILDIZ[3,*], Remzi GÖREN[4], Ömer ELİTOK[5]

[1]Department of Mining Engineering, Faculty of Engineering, Afyon Kocatepe University, 03100 Afyonkarahisar, Turkey
[2]Department of Physics, Anadolu University, 26470 Eskişehir, Turkey
[3]Department of Geological Engineering, Faculty of Engineering, Afyon Kocatepe University, 03100 Afyonkarahisar, Turkey
[4]Department of Materials & Ceramics Engineering, Faculty of Engineering, Dumlupinar University, 43100 Kütahya, Turkey
[5]Department of Geological Engineering, Faculty of Engineering, Süleyman Demirel University, 32260 Isparta, Turkey

Received: 31.12.2011 • **Accepted:** 04.12.2012 • **Published Online:** 13.06.2013 • **Printed:** 12.07.2013

Abstract: Lens-shaped talc deposits related to Mesozoic gabbroic rocks are exposed in an area of 2 km^2, about 80 km northwest of Afyonkarahisar (western Anatolia). Different alteration zones in talc deposits were determined depending on differences related to the texture and color of the host rock. In order to determine mineralogical, geochemical, and physicochemical features of the Emirdağ talc deposits, X-ray diffractometer, scanning electron microscope (SEM), FT-IR and Mössbauer spectroscopy, differential thermogravimetric analyses, BET-specific surface area, color, water soluble substance, acid–soluble carbonate, and acid–soluble iron tests were performed on the samples collected from different alteration zones in the lateral direction. Four groups of mineral paragenesis were determined: i) talc and chlorite-bearing actinolite (E1), ii) actinolite-rich talc (E-2), iii) chlorite and calcite-bearing talc (E-3), and iv) pure talc (E-4). Talc, actinolite, and chlorite are dominant. SEM analyses show that fine shreds, like microcrystalline talc crystals, are associated mainly with actinolite and chlorite, and actinolites are mainly transformed into chlorite and talc. Ni and Cr contents of the Emirdağ talcs are consistent with the composition of the talc deposits formed in relation to ultramafic rocks. Energy dispersive X-ray spectrometry, chemical analysis, and Mössbauer spectroscopy results show that iron in the Emirdağ samples was mainly derived from talc minerals and this iron occurs as Fe^{+2} in the crystal lattice structure of talc. Because removal of iron from Emirdağ talc seems difficult during mineral processing techniques, the Emirdağ talc can be used in its crude state in the cosmetic, paint, and paper industries as a secondary raw material.

Key words: Talc, mineralogy, FT-IR, Mössbauer spectroscopy, thermal analysis, industrial usage, Afyonkarahisar

1. Introduction

Talc is an industrial raw material used in many industrial applications because of its unique physical and chemical features. It is a layered, hydrous magnesium silicate with the chemical formula of $Mg_3(Si_2O_5)_2(OH)_2$ and the theoretical chemical composition of 63.5 wt.% of SiO_2, 31.7 wt.% of MgO, and 4.8 wt.% of H_2O (Grim 1968). Talc extracted from various localities shows different mineralogical, chemical, and physical properties; these features depend on their parent rock types, and origins play a key role in their usability. Based on their origins, talc deposits can be classified into 5 groups: i) ultramafic-related talc deposits, ii) talc deposits within dolomites, iii) metamorphic talc deposits, iv) talc deposits related to banded iron formations, and v) secondary talc deposits (Prochaska 1989). While the first 2 of these are mined economically, the other talcs do not have the characteristics needed in industry. Moreover, metamorphism is effective on all types except for the last.

The main properties of talc can be listed as follows: hydrophobicity, organophilicity, platyness or lamellarity, softness, chemical inertness, high thermal stability, low electrical conductivity, heat resistance, wide particle size distribution, high specific surface area, oil absorption, and surfactant/polymer absorption capability (Van Olphen 1977; Sanchez-Soto *et al.* 1997; Tomaino 2000; Lopez-Galindo & Viseras 2004; Pérez-Maqueda *et al.* 2004; Nkoumbou *et al.* 2008a; Wallqvist *et al.* 2009). As a result of these characteristics, talc is used in numerous industrial applications including cosmetics, pharmaceuticals, pesticides, paper, food, plastics, ceramics, paint, and textiles, as reviewed in the literature (Bizi *et al.* 2003; Lopez-Galindo & Viseras 2004; Martin *et al.* 2004; Terada & Yonemochi 2004; Gören *et al.* 2006; Neto & Moreno 2007).

* Correspondence: ayildiz@aku.edu.tr

According to State Planning Organization (DPT) statistics, Turkey has 482,736 t of talc reserves. The most important talc deposits in Turkey occur in the Sivas, Balıkesir, Aydın, Kütahya, Karaman, Bolu, Bursa, Sakarya, and Afyonkarahisar regions (DPT 2007). Talc deposits formed from the alteration of ultramafic rocks are found in the Sivas, Kütahya, Karaman, and Afyonkarahisar regions (Murat & Temur 1995; Yalçın & Bozkaya 2006). The other talc deposits related to metamorphic rocks occur in Balıkesir, Aydın, and Afyonkarahisar (MTA 1980; Çoban 2004). Nearly 2000 t of talc are produced per year in the Sivas, Balıkesir, Aydın, Kütahya, and Eskişehir regions. Since the annual talc production of the country did not meet the domestic market, the annual talc import of Turkey is higher than the domestic production. Even though there are enough talc deposits for domestic industry, the reasons for the low domestic talc production, and hence demand for talc import, can be interpreted as being insufficient investigation of the geological, mineralogical, and geochemical features. The Turkish paint industry is the main consumer of high quality and very fine-grained (<5 μm) talc. In contrast, the major problem with Turkish talc deposits is that they are mostly not suitable for the paint industry, which requires high-quality whiteness, brightness, and very low Fe content.

The Emirdağ talc deposit is located about 80 km north of Afyonkarahisar in western Anatolia and covers an area of nearly 2 km^2 (Figure 1). Talc produced from the Emirdağ deposit with an annual mine production of 500 t until 2005 has been used in the domestic market as a plastic filling material, but its domestic consumption has been limited due to insufficient investigations on the geological features of talc deposits and mineralogical, geochemical, and physical features of the talc minerals. Moreover, quality problems arose for the produced talc ores. In this study, the aim is to i) investigate geological features of the talc deposits; ii) identify mineralogical, geochemical, physicochemical features of the talc mineral; and iii)

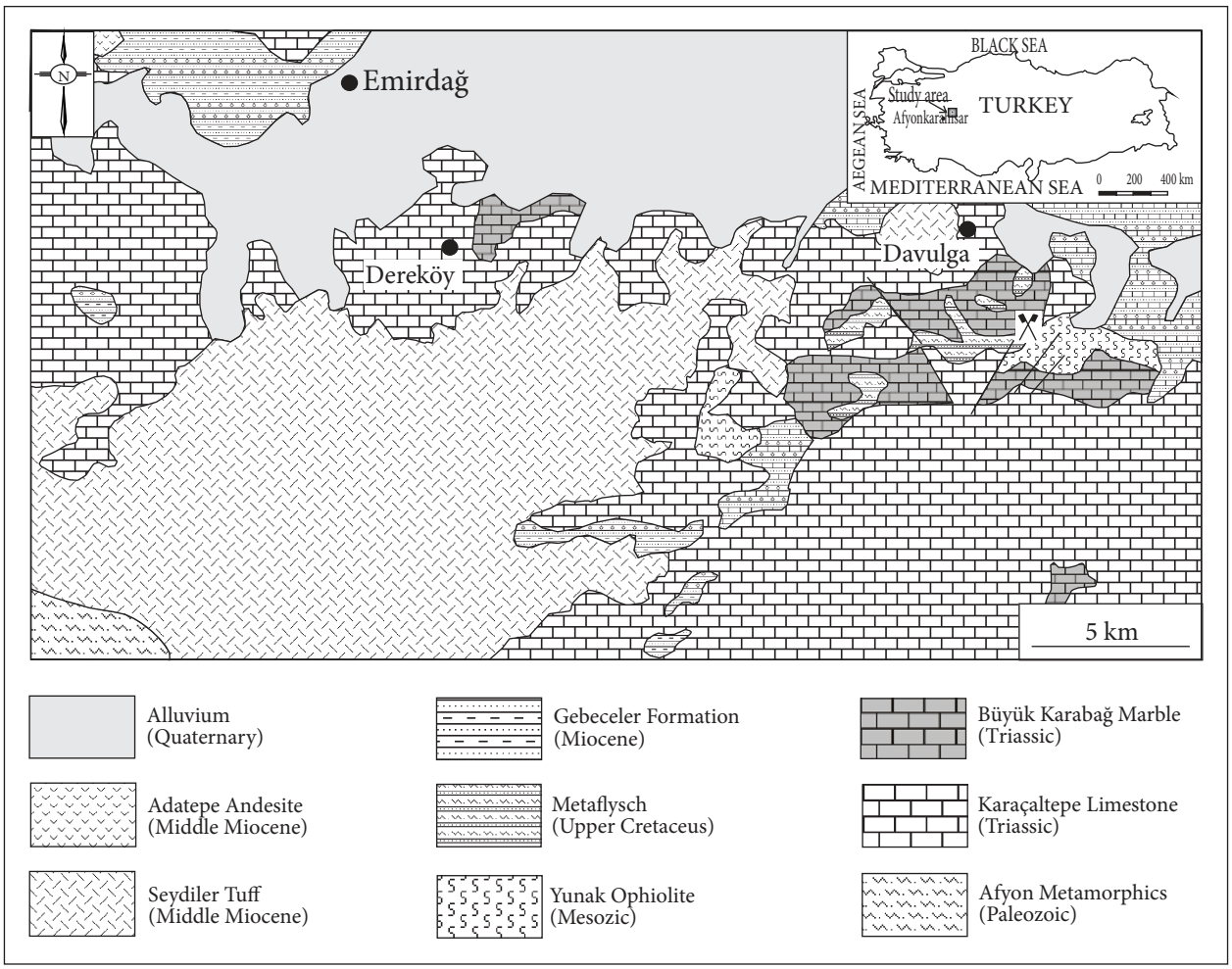

Figure 1. The geological map of the study area (Turhan 2002).

determine potential uses of talc. This study is important in terms of economic production of the Emirdağ talc deposit since it is close to industrial cities such as Kütahya, Uşak, Bilecik, Eskişehir, and Ankara.

2. Geological setting

The Paleozoic Afyonkarahisar metamorphics constitute the basement rocks in the study area (Figure 1). Metin *et al.* (1987) reported that the unit comprises a variety of schists, metasandstones, and metaconglomerates, with some lenticular marble horizons. The basement rocks are covered unconformably by Triassic Karacaltepe limestone and Büyük Karabağ marbles (Kibici *et al.* 2000). Mesozoic Yunak ophiolite is associated with Büyük Karabağ marbles with tectonic boundary. Yunak ophiolite consists of gabbro slice displaying foliation and cataclastic texture toward the bottom. The brown-colored metaflysch consists mainly of conglomerate, sandstone, siltstone, and sandy limestone and occasionally shows features of olistostrome. The Gebeceler formation of Miocene age, which comprises intercalation of sandstone, siltstone, marl, and the Seydiler tuff of the Middle Miocene, spreads unconformably on the metaflysch. The final stage of volcanism yielded the Adatepe andesite of the Middle Miocene. The Emirdağ-Afyonkarahisar talc deposits have been formed by the alteration of the gabbro along joints and fault planes. Based on differences in the texture and color of the parent rocks, 5 alteration zones were distinguished. These are: i) fresh rock of gabbroic composition, ii) green-colored actinolite zone, iii) talc level, iv) amber-colored altered zone, and v) dark brown-colored altered zone. Talc deposits occur as lens-shaped pockets and sheet-like bodies in different extensions and directions.

3. Analytical methods

E-1 samples were collected from the actinolite zone, and E-2, E-3, and E-4 samples were also gathered from the different layers along the lateral direction of the talc level in the Emirdağ deposit in the Afyonkarahisar region. The samples were crushed in a jaw crusher and milled to less than 40 μm in size. The samples were then homogenized. Mineralogical and physicochemical analyses were performed on the representative samples.

3.1. Mineralogical and petrographical investigations

Mineralogical investigations were performed by X-ray diffraction (XRD) with a Shimadzu XRD-6000 model diffractometer with a Ni filter and CuKα radiation on random and oriented samples. The diffraction patterns were recorded between 2° and 70° (2θ) at a scanning speed of 2° (2θ)/min. Bulk mineralogy was determined on random powders. Clay mineralogy was determined by separation of the fraction of less than 2 μm with sedimentation. Measurements were carried out on samples that were air-dried, ethylene glycol-solvated, and heated to 550 °C (Brown 1972). Mineral abundances of samples were determined by interpretation of XRD data. The procedure of this method was described by Chung (1974). The error margin of this method is approximately 10%.

Morphological and microchemical analyses were carried out using a LEO VP-1431 scanning electron microscope with an energy dispersive X-ray spectrometer (SEM-EDX). Before the SEM analysis, samples were coated with a thin film (thickness: 25 nm) of gold using a sputter coater to make the sample conductive.

3.2. Geochemical analyses

The chemical compositions of the samples were determined with an X-ray fluorescence (XRF) spectrometer (Bruker, S8 Tiger WDXRF). Prior to the chemical analysis, 1.5 g of samples and 7.5 g of $Li_2B_4O_7$ were mixed in platinum crucibles, and then these mixtures were melted in a fusion device at 1300 °C to obtain glass pellets.

The substitution in the unit cell and the position of iron in the E-3 talc sample was examined by Mössbauer spectroscopy. For this purpose, the ^{57}Fe Mössbauer spectrum was obtained at room temperature (300 K) with a conventional constant acceleration mode using a 10 mCi ^{57}Co radioactive source (diffused in Rh). A Normos-90 computer program was used to determine the Mössbauer parameters. The solid line in the spectrum represents computer-fitted curves, and dots represent the experimental points. The velocity scale (±9 mm/s) is calibrated with metallic iron foil absorber, and isomer shift (IS) is given with respect to the center (at 0 mm/s) of this spectrum.

Fourier transform-infrared (FT-IR) spectra of powdered samples were recorded using the Bruker IFS-66 series. The infrared spectrum range was 4000–400 cm^{-1}. Samples of 2 mg were thoroughly mixed with 200 mg of spectroscopic grade KBr in an agate mortar. The mixtures were placed in a hydraulic press and compressed to produce pellets for recording the spectra. The spectra of samples were recorded by accumulating 34 scans at 2.0 cm^{-1} resolution.

Differential thermal and thermogravimetry analyses (DT/TGA) of the samples were carried out with a Setaram Setsys Evaluation simultaneous thermal analysis apparatus. The samples were heated in an Al_2O_3 crucible in the temperature range of 30–1250 °C with a heating rate of 10 °C min^{-1} in a nitrogen atmosphere. About 25 mg of the samples was used in each run.

3.3. Physicochemical analyses

The specific surface area of the samples was measured using a nitrogen gas absorption method (BET technique, Quantachrome Instruments, NOVA 2200e). Prior to the analysis, the samples were kept in a vacuum (10^{-3} Torr) at 120 °C for 8 h. Samples were run in duplicate. Details

of sample preparation and applications for the source and special clays were presented previously (Doğan *et al.* 2006). To determine the color properties of the materials, L^*, a^*, and b^* values and whiteness index (WI) were measured under the standard illuminant D65 by using the CIELAB system (CM-700d Konica Minolta Series Spectrophotometer). The spectrophotometer was calibrated to the perfect white diffuser by a ceramic plate with tristimulus values $X = 90.3$, $Y = 92.1$, $Z = 105.7$ and chromaticity coordinates $x = 0.3135$, $y = 0.3196$. The pH, water soluble substance, acid-soluble carbonate, and acid-soluble iron of the samples were determined according to the Turkish Standards adapted to European Norms TS EN ISO 3262-10 and other Turkish Standards TS 2973 and TS 10521.

4. Results and discussion

4.1. Mineralogy and petrography

XRD analysis showed that the Emirdağ samples consist mainly of talc, chlorite, and actinolite, with minor amounts of calcite (Figure 2). Studied samples were classified into 4 groups based on the results of semiquantitative analysis: i) (E-1): talc and chlorite bearing actinolite (calcite 1%, talc 10%, chlorite 19%, and actinolite 70%), ii) (E-2): actinolite-rich talc (chlorite 5%, actinolite 25%, and talc 70%), iii) (E-3): chlorite bearing talc (calcite 5%, chlorite 10%, and talc 85%), and iv) (E-4): pure talc (actinolite 5% and talc 95%) (Table 1). The mineralogy of Emirdağ talc was similar to the ultramafic hosted-talc occurrences of Sivas (Turkey) (Yalçın & Bozkaya, 2006); the Wadi Thamil, Rod Umm El-Farag (El-Sharkawy 2000), and Athshan (Schandl *et al.* 1999) areas (Egypt); and the ultramafic talc deposits of Austria (Prochaska 1989). XRD data indicate that the 2q value and crystal plane (*hkl*) values of the most important 3 peaks from talc were as follows: ~9.40° (001), 18.95° (002), and 28.55° (003). Talc was distinguished from pyrophyllite and minnesotaite minerals by their $d_{(002)}$-spacings. Talc exhibits $d_{(002)}$-spacing at 9.30 Å, whereas the $d_{(002)}$-spacings of pyrophyllite and minnesotaite are 9.16 Å and 9.53-9.60 Å, respectively (Thorez 1976). The $d_{(001)}$-spacing of talc was not changed by ethylene glycol (EG) or heat treatments at 550 °C (Figure 3). According to Moore and Reynolds (1997), the dehydroxylation is only observed in talc due to high temperature treatments.

The SEM studies revealed that actinolite and chlorite crystals accompany talc. Tabular, prismatic, acicular, and fibrous actinolite crystals are common in E-1 samples (Figures 4a and 4b). Actinolites are slightly altered to chlorite. Chlorite occurs in the form of curved flakes with angular borders and is randomly distributed along the edge of actinolite crystals. The semiquantitative EDX analyses show the releasing of Si and Ca and enrichment of Mg, Fe, and Al during the conversion of actinolite to chlorite. The talc particles occur in fine shreds, plates, and flakes

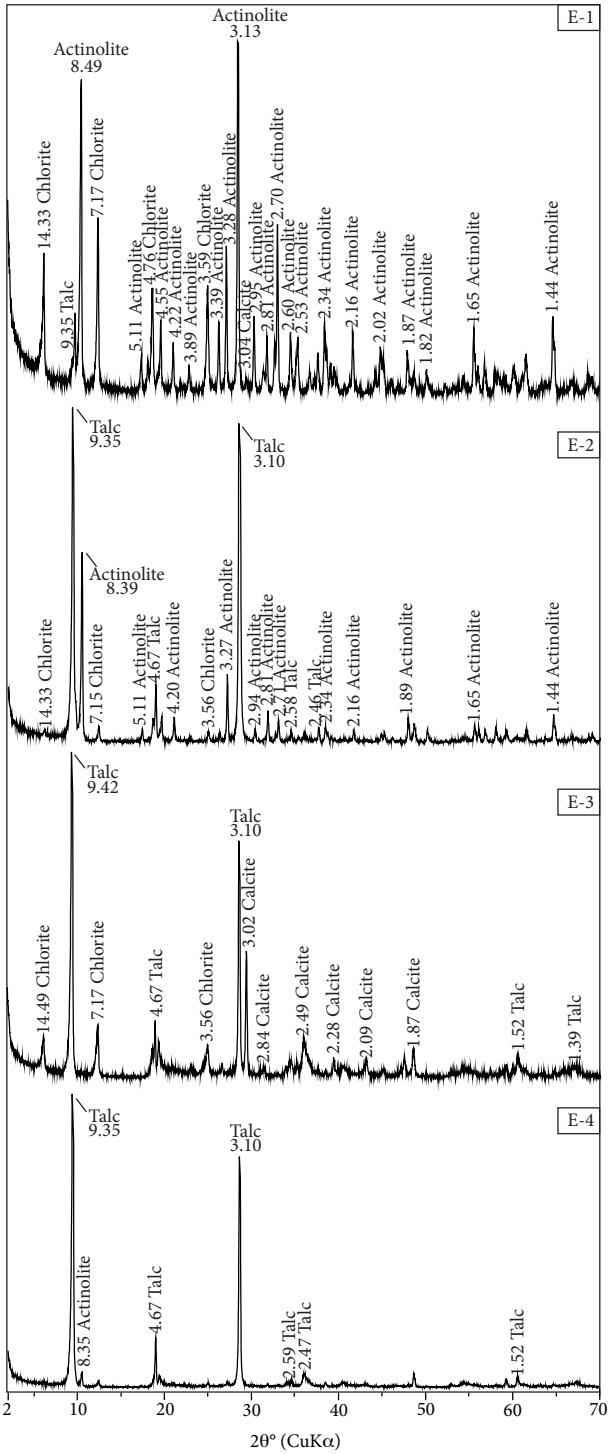

Figure 2. Representative XRD patterns of unoriented samples from Emirdağ.

with differently sized and layered crystals. The actinolite was replaced by pseudomorphic talc crystals in the E-2 and E-4 samples (Figures 4c–4f). Depletion of Fe and Ca and enrichment of Mg and Si should be evidenced by

Table 1. Semiquantitative analysis results (wt.%) of talc samples from Emirdağ.

Sample	E-1	E-2	E-3	E-4
Talc	10	70	85	95
Chlorite	19	5	10	0
Actinolite	70	25	0	5
Calcite	1	0	5	0

comparison of chemical analyses of both fresh and altered samples. According to EDX analyses, talc is composed mainly of Si (71.0–73.5 wt.%), Mg (21.0–22.0 wt.%), and Fe (5.0–6.4 wt.%).

Individual talc grains have a grain width diameter of 6–14 μm and an average thickness of less than 0.5 μm in all samples (Figures 4c–4f). Thus, Emirdağ talc may be classified as microcrystalline talc due to its relatively low basal/edge surface ratio. According to the literature, platy talc can be classified as microcrystalline or macrocrystalline (Ciullo & Robinson 2003; Ferrage *et al.* 2003). Microcrystalline varieties are naturally small in plate size and comprise compact, dense mineral particles. Macrocrystalline varieties contain relatively large plates with higher aspect ratio (high basal/edge surface ratio). The grinding of microcrystalline talc is easier than that of macrocrystalline talc (Ferrage *et al.* 2003). The morphology (e.g., basal/edge surface ratios, degree of delamination) of talc particles as layered clay minerals plays a decisive role in its usability as a filler material, especially in plastic, coating, and paint industries (Yuan & Murray 1997; Ciullo & Robinson 2003; Ferrage *et al.* 2003) and also on its wettability and flotation behavior (Hiçyilmaz *et al.* 2004). For example, kaolin used in paper sludge and the spherical halloysite (both kaolinite and halloysite have 1:1 types of layer structures; halloysite usually contains some interlayer water) showed the lowest viscosity, followed by platy kaolinite and tabular halloysite (Yuan & Murray 1997). This indicates that the morphology of filler particles directly affects the rheological behavior of their suspension and, in turn, their usability. The morphology of talc particles is dependent on different factors, such as geological formation conditions of talc deposits (Ciullo & Robinson 2003; Nkoumbou *et al.* 2008b), particle size, grinding method, and conditions (Sanchez-Soto *et al.* 1997; Ferrage *et al.* 2003; Hicyilmaz *et al.* 2004; Ulusoy 2008).

4.2. Geochemical properties

The results of chemical analyses of the Emirdağ samples are presented in Table 2. Emirdağ talcs are characterized by high SiO_2 (44.35–59.56 wt.%) and MgO contents (24.08–28.88 wt.%). Fe_2O_3 and TiO_2 contents, which significantly affect the color and brightness of minerals such as talc and kaolinite minerals (Bundy & Ishley 1991), were 5.40–6.10 wt.% and 0.15 wt.%, respectively (Table 2). One of the characteristic features of Emirdağ talcs is their low Al_2O_3 content (0.49–3.29 wt.%). Ni, Cr, and Co are important elements for the identification of origin of talcs. Their abundances are low in Mg-carbonatic talc, but are concentrated in ultramafic talcs (Prochaska 1989). The Emirdağ talc deposit is related to ultramafic rocks due to its high Ni (2100–2600 ppm), Cr (2000–3500 ppm), and Co (82.50–84.00 ppm) contents. In terms of Ni, Cr, and Co, the Emirdağ talc deposits are similar to the ultramafic-related talc deposits in the Sivas (Yalçın & Bozkaya 2006) and Karaman (Murat & Temur 1995) regions, but differ from Gümeli-İvrindi talcs (Balıkesir, Turkey; Çoban 2004).

In terms of the cosmetics and pharmaceutical industries, the concentrations of toxic elements such as Pb, As, and Hg in Emirdağ talc samples are within acceptable levels (TS 2973). On the other hand, some trace elements, such as Co, Cu, Zn, and Zr may be beneficial, particularly for the use of talc in medical applications such as skin care and mud baths (Olabanji *et al.* 2005). Taking into account the mineralogical, petrographical, and geochemical data (Table 1, Figure 4, and Table 2), the following results were obtained: i) Fe_2O_3 and Al_2O_3 ratios in talcs are directly proportional to their chlorite contents, ii) the nonexistence of secondary iron mineral in Emirdağ samples and the similarity between the Fe_2O_3 contents in EDX and chemical analyses indicate structural iron in Emirdağ talcs, and iii) the CaO content is related to the existence of actinolite mineral in E-1, E-2, and E-4 samples, whereas the CaO content in E-3 sample results from calcite.

Iron content is an effective parameter in the use of talc. Therefore, the percentage of iron, its origin (i.e. from crystal structure or from other iron-bearing minerals), and its valence forms are important. To determine these features, in addition to mineralogical, petrographical, and chemical analyses, Mössbauer analysis was performed. Using Mössbauer analysis, the origin of iron was investigated for the chlorite-bearing talc sample (E-3), which has high talc content. Figure 5 shows the Mössbauer spectrum of the talc at room temperature (approximately 300 K). It should be noted that the isomer shift (IS) is the shift of the centroid of the spectrum from zero velocity and is given

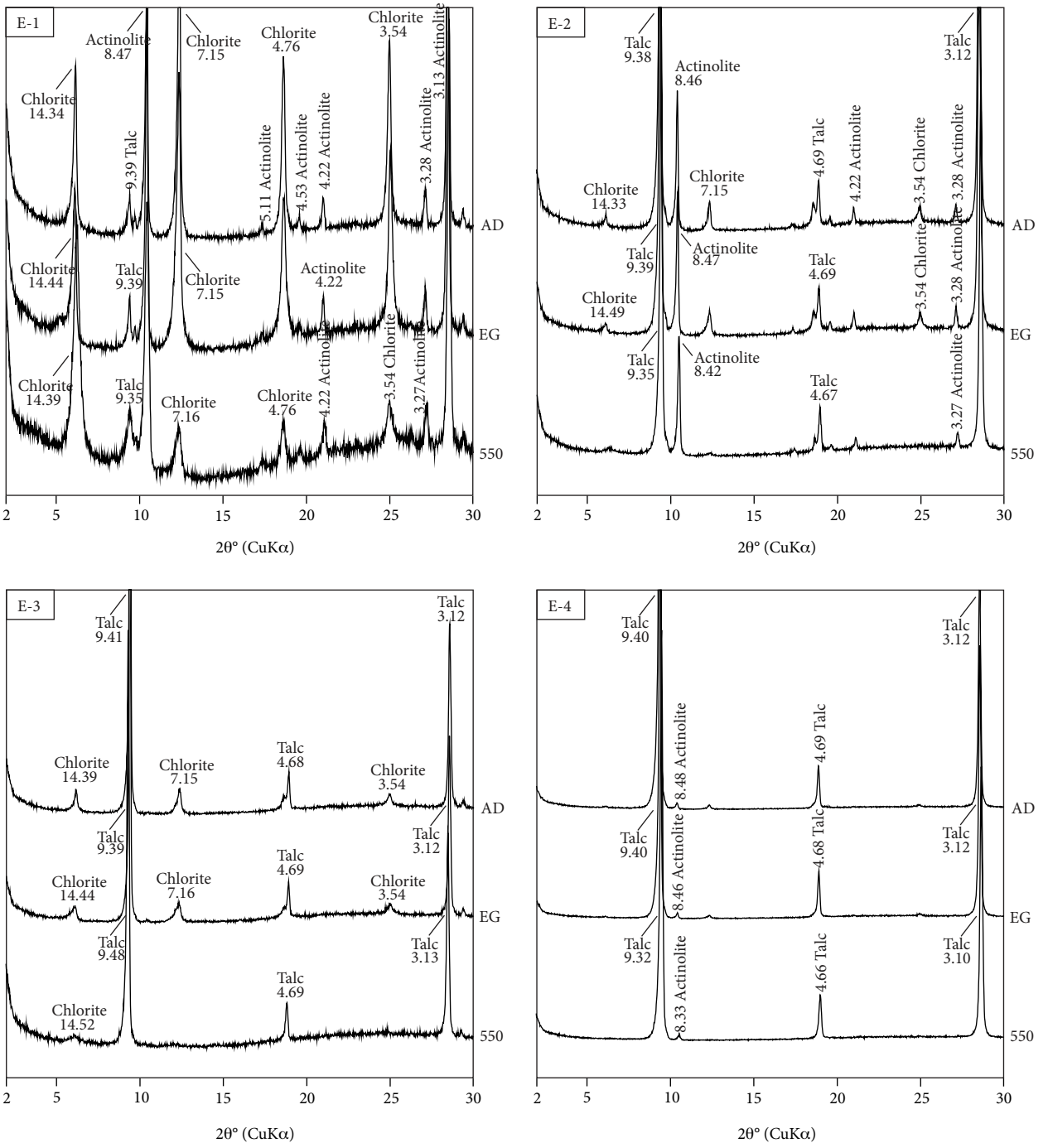

Figure 3. Representative XRD patterns of Emirdağ talcs. Key to the symbols: AD, air-dried; EG, ethylene glycolated; 550, heated at 550 °C.

relative to either the source or some standard material. In the case of ^{57}Fe, it is usually metallic iron. The quadrupole splitting (QS) is the separation of the 2 lines of a ^{57}Fe doublet. Both IS and QS are customarily given in terms of the source velocity in mm/s (Murad 2006; Gill *et al.* 2011). According to Rancourt's (1998) Mössbauer parameters (in clay samples), IS values are in the range of ≈1.0–1.3 mm/s and QS values are in the range of ≈1.5–3.0 mm/s for Fe^{+2} cations (ferrous). On the other hand, IS values are in the range of ≈0.2–0.4 mm/s and QS values are in the range of 0.0–1.5 mm/s for Fe^{+3} cations (ferric). The results obtained from the Mössbauer parameters of E-3 talc show

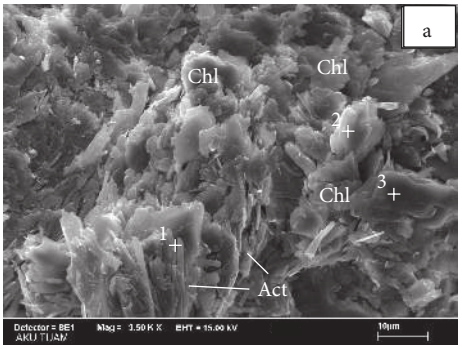

Oxides (%)	Spectrum 1	Spectrum 2	Spectrum 3
MgO	17.7	20.5	18.9
SiO_2	51.2	45.2	43.4
Fe_2O_3	13.8	14.9	18.9
CaO	4.1	1.7	0
Al_2O_3	13.2	17.7	18.9

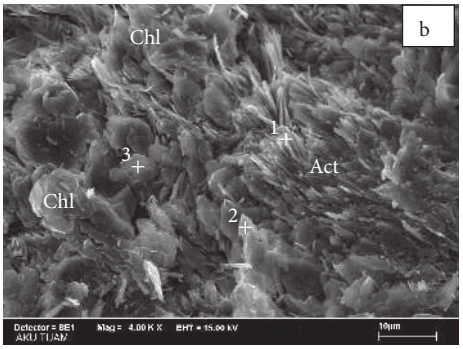

Oxides (%)	Spectrum 1	Spectrum 2	Spectrum 3
MgO	17.7	22.6	23.8
SiO_2	57.3	43.0	44.0
Fe_2O_3	7.8	14.9	10.8
CaO	9.0	1.6	1.1
Al_2O_3	8.2	13.6	20.3

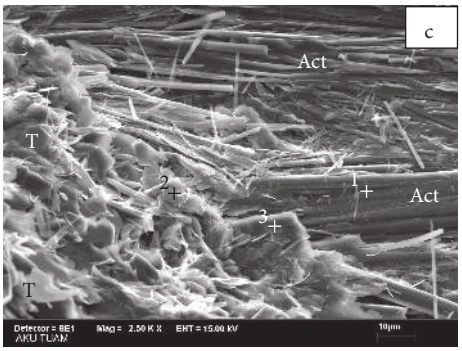

Oxides (%)	Spectrum 1	Spectrum 2	Spectrum 3
MgO	16.3	12.6	14.7
SiO_2	65.5	79.5	78.8
Fe_2O_3	5.3	5.8	6.6
CaO	13.0	2.2	0

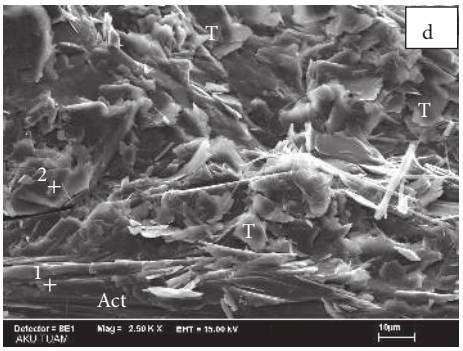

Oxides (%)	Spectrum 1	Spectrum 2
MgO	21.8	21.4
SiO_2	71.0	73.5
Fe_2O_3	5.2	5.1
CaO	2.0	0

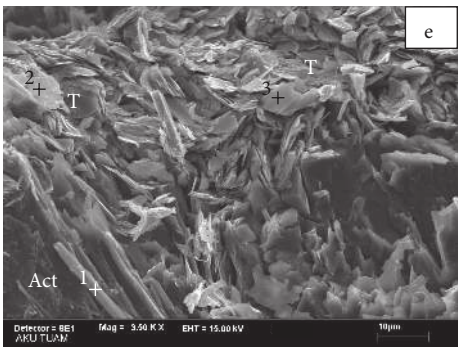

Oxides (%)	Spectrum 1	Spectrum 2	Spectrum 3
MgO	16.2	21.5	21.0
SiO_2	66.9	72.6	72.6
Fe_2O_3	8.3	5.9	6.4
CaO	8.5	0	0

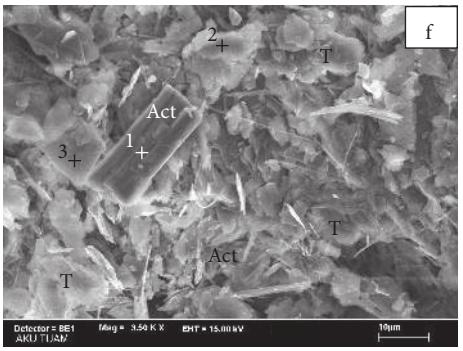

Oxides (%)	Spectrum 1	Spectrum 2	Spectrum 3
MgO	15.0	21.6	22.0
SiO_2	64.7	71.0	73.0
Fe_2O_3	6.6	6.1	5.0
CaO	13.7	1.3	0

Figure 4. Scanning electron micrographs and semiquantitative EDX results of Emirdağ talcs. (a) and (b): Tabular, prismatic, acicular, fibrous-shaped actinolite crystals and curved chlorite flakes. (c), (d), (e), and (f): Differently sized layered talc crystals occur in fine shreds, plates, and flakes. Key to the symbols: Act, actinolite; Chl, chlorite; T, talc.

Table 2. Chemical analysis of the Emirdağ talc samples.

Components in wt.%	E-1	E-2	E-3	E-4
SiO_2	50.93	56.76	44.35	59.56
Al_2O_3	3.44	0.76	3.29	0.49
Fe_2O_3	6.63	5.62	6.10	5.40
MgO	22.25	24.08	27.08	28.88
CaO	10.77	9.37	6.18	0.58
MnO	0.32	0.17	0.11	---
K_2O	---	0.02	0.09	---
Na_2O	0.33	---	---	---
TiO_2	0.26	---	0.15	---
Cr_2O_3	0.12	0.20	0.28	0.35
NiO	0.21	---	0.21	0.26
P_2O_5	---	---	0.04	---
LOI	4.63	3.02	11.94	4.60
Total	99.89	100.00	99.82	100.12
Trace elements in ppm				
Co	82.50	82.80	83.60	84.00
Cu	13.20	6.80	4.70	5.20
Zn	23.00	8.21	4.00	4.83
Zr	29.90	10.68	0.60	0.92
Pb	6.70	5.11	4.60	4.75
As	0.50	0.50	<0.5	<0.5
Hg	<0.01	<0.01	<0.01	<0.01

LOI: Loss on ignition

that the IS and QS values were centered around 1.26 mm/s and 2.72 mm/s, respectively. The IS and QS values of talc and chlorite are in good agreement with values reported earlier. Gonçalves *et al.* (1991) found that QS = 2.66 mm/s and 1.15 mm/s corresponded to Fe^{+2} present in talc and chlorite at room temperature. The high values of IS and QS are thus characteristic of iron in the crystal structure of talc and chlorite in our sample. Similar Fe_2O_3 contents obtained from chemical and EDX analyses of pure talc sample (E-4) (Figures 4c–4f) also confirm the occurrence of iron in the crystal structure of talc mineral.

Infrared spectroscopy has been used successfully in the characterization of inorganic compounds as well as organic compounds (Stuart *et al.* 1998). Figure 6 shows the FT-IR spectra of the Emirdağ samples (E-1, E-2, E-3, and E-4) used in this study. According to the characteristic IR frequencies of talc reported by other researchers (Wilkins & Ito 1967; Ferrage *et al.* 2003; Nkoumbou *et al.* 2008b), the absorption bands located at 3677, 3661, and 3643 cm^{-1} are the fundamental OH stretching vibrations arising from νMg_3O–H, νMg_2FeO–H, $\nu MgFe_2O$–H, and νFe_3O–H, respectively. It is clearly seen that the peak intensity decreases with decreasing talc content in the sample. Existence of the peaks stated above indicates the occurrence of iron in the crystal structure of talc. The observed strong band at around 1040 cm^{-1} is assigned to the out-of-plane symmetric stretching of ν_3Si-O-Si groups of talc (Farmer 1974; Wang & Somasundaran 2005). Another sharp absorption at 669 cm^{-1} is due to the stretching vibration of Si-O-Mg in talc structure. The intensity of 2 peaks belonging to talc show the decreasing of talc content and widening of peaks, similar to that given above. The 2 peaks in the spectra of the E-1 and E-3 samples appeared at 3588 and 3435 cm^{-1} because of the OH stretching vibration in the hydroxide layer of chlorite (Sontevska *et al.* 2007). The 3 bands in the spectrum of the E-3 sample appearing at around 1424 cm^{-1} (strong), 875 cm^{-1} (shoulder), and 715 cm^{-1} (weak) are assigned to the

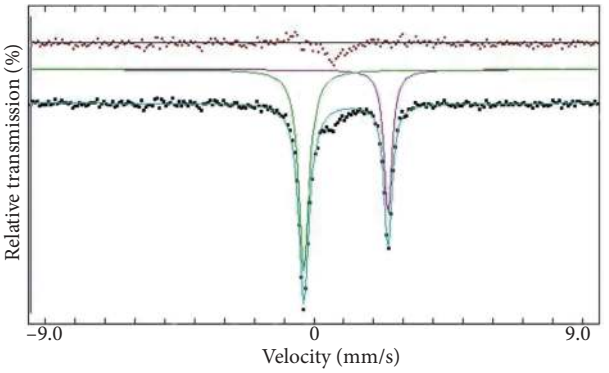

Figure 5. Mössbauer spectrum of talc sample E-3.

characteristic CO_3 vibration of calcite. The other 2 medium bands located at 1790 and 2512 cm^{-1} are also assigned to calcite (Wilson 1995; Shoval 2003; Xie *et al.* 2006). In the IR spectrum of talc- and chlorite-bearing actinolite (E-1) and actinolite-rich talc (E-2), the strong peak at 750 cm^{-1} and small peaks in the range of 923–1106 cm^{-1} belong to actinolite mineral (Van Der Marel and Beutelspacher 1976).

Differential thermal analysis (DTA) determines the temperature at which thermal reactions, such as phase transformation and thermal decomposition, take place in a material when it is heated continuously to an elevated temperature, and also the intensity and general characters (endothermic or exothermic) of such reactions (Speyer 1994). In contrast, thermogravimetric (TG) analysis determines the weight gain or loss of a material (e.g., minerals, glasses, ceramics, polymers) due to absorption or gas release as a function of temperature. DTA and TG curves of the talc sample are shown in Figures 7a and 7b. The DTA and TG curves indicate different temperature ranges at which the mass losses accompanying 4 endothermic reactions occurred. On the DTA curve of the talc- and chlorite-bearing actinolite (E-1) and chlorite-bearing talc (E-3) samples, endothermic peaks were observed in the temperature ranges of 500–600 °C and 760–780 °C (Figure 7a), and hence mass loss (Figure 7b) resulted from the dehydroxylation reaction of chlorite (Nkoumbou 2006). It was observed that these endothermic peaks disappeared with increasing talc contents in the samples. The endothermic peak of pure talc samples (with 95 wt.% talc content) at a temperature of 895 °C and mass loss indicate transformation of talc to enstatite ($MgSiO_3$) and silica minerals (SiO_2) (Nkoumbou 2006). The endothermic peak observed for sample E-1 (containing about 70% actinolite) around 1220 °C resulted from deformation of the crystal structure of actinolite (Taboadela & Aleixandre Ferrandis 1957). The highest mass loss occurred in sample E-3, which probably resulted from calcite content. Mass loss (~5 wt.%) occurred in sample E-3 between the

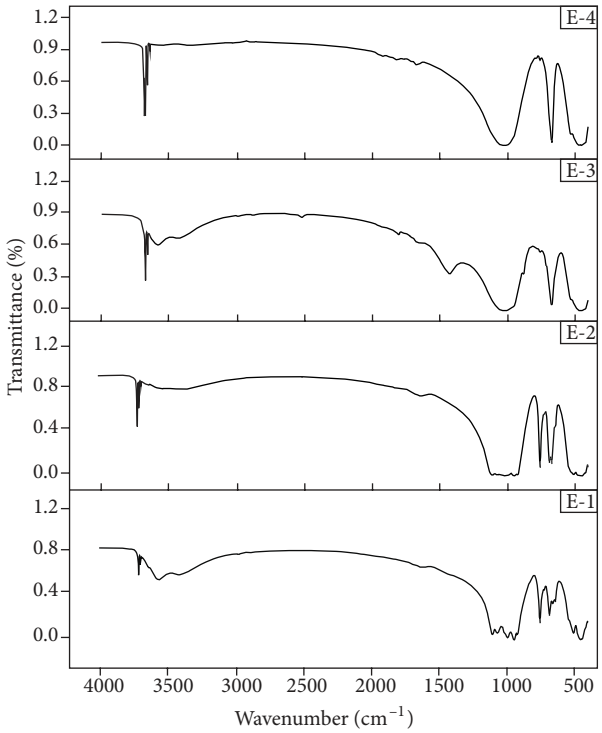

Figure 6. FT-IR spectra of the talc samples.

temperatures of approximately 650 and 800 °C, and this resulted from CO_2 gas that was removed from the structure after the thermal decomposition of calcite. Consistent with this, on the DTA curve of the same sample, endothermic peaks from 760 to 895 °C confirm this situation. Similar results were obtained in thermal analyses performed using various solids containing pure calcite (Hristova & Jancev 2003; Hojamberdiev *et al.* 2008). The total mass loss values of the samples (Figure 7b) are corroborated by the loss on ignition yielded by the chemical analysis (Table 2).

4.3. Physicochemical properties

BET-specific surface areas of the powdered talc samples were recorded between 6.65 and 11.87 $m^2 g^{-1}$ (Table 3). Among the samples, the lowest specific surface area was measured for sample E-4 with high talc content. Comparing BET values of source and specific clays of US Geological Survey geological standards, the values obtained from the talc used in this study are close to the values obtained from these clay standards (Doğan *et al.* 2006).

The pH values of talc suspensions are close to each other and in the range of standards (TS EN ISO 3262-10). The amount of dissolved material in water should be as much 0.2 wt.% for the talc that will be used in the paint (TS EN ISO 3262-10) and cosmetic (TS 2973) industries. In this study, the amount of dissolved material of the talc samples in water varies between 0.13 and 0.17 wt.%. Of these, sample E-3 containing calcite has the highest amount of

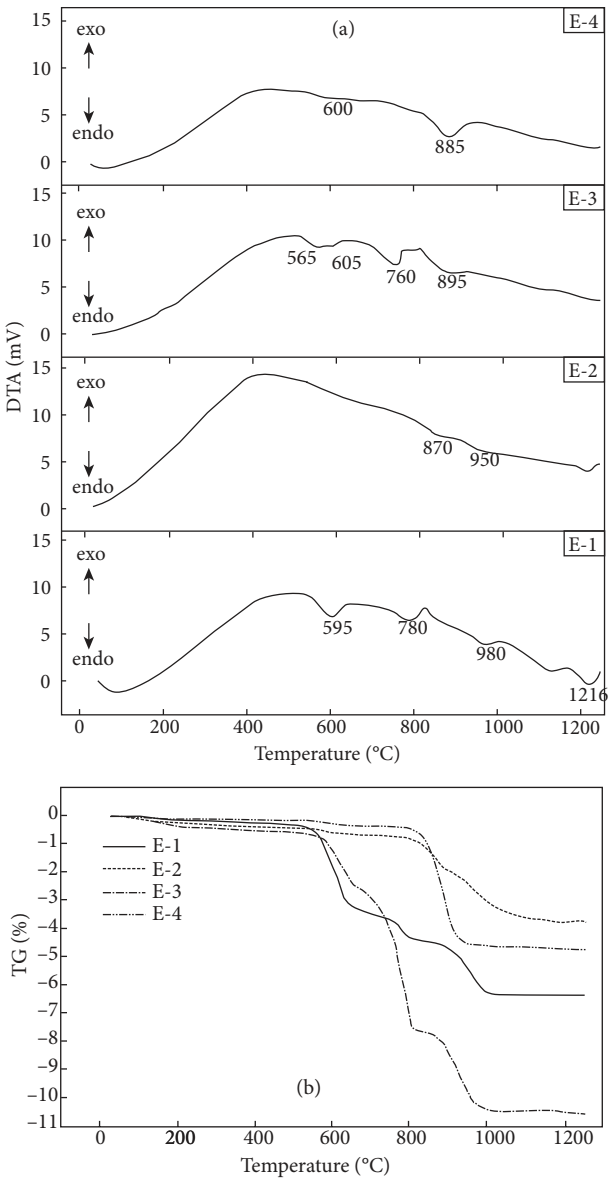

Figure 7. (a) DTA and (b) TG curves of the talc samples.

dissolved material. On the other hand, the amount of iron dissolved in acid is as much as 0.66 wt.% from sample E-1, which also contains the highest iron (Table 2). The lowest dissolved material in acid with 0.54 wt.% is sample E-4, containing 95 wt.% talc. Based on the dissolved material in acid, the Emirdağ talc samples exceed the maximum value (0.5 wt.%) given for the primary quality raw material (TS 10521) in the paper industry. However, they are lower than the maximum value (75 wt.%) given for the cosmetics industry (TS 2973).

The color properties were measured as L^*, a^*, b^*, and WI parameters, which are calculated from the X, Y, Z tristimulus values (Billmeyer & Saltzman 1981). These parameters are statistically related to the chemical and mineralogical composition of the sample. In the CIELAB system, L^* is the degree of lightness and darkness of a color in relation to a scale extending from white (L = 100) to black (L = 0). Parameter a is a scale extending from green (–a) to red (+a), and b is a scale extending from blue (–b) to yellow (+b). Table 3 shows the results of color analysis (L^*, a^*, b^*, WI) performed on the Emirdağ talc samples. The WIs of samples E-1, E-2, E-3, and E-4 were measured as 76.19, 81.96, 85.43, and 89.16, respectively. As is known, the whiteness of talcs directly affects their utility in cosmetics, paint, and paper industries (Soriano *et al.* 2002). The whiteness of all of the talc samples is under the desired values when compared with standards (TS 2973; TS 10521; TS EN ISO 3262-10). The WI and L values proportionally increase with increasing talc contents and decrease with decreasing iron and titan elements causing color. The same results were reported by Soriano *et al.* (2002), who studied relations between color and mineral/chemical compositions of the industrial talcs from different countries. Consequently, impurity ratio and iron content would seem to be influential variables in the color variations in the samples. Mineralogically and chemically pure talc is white, but greenish, bluish, brownish, or reddish varieties have also been described. Furthermore, the accessory minerals are frequently yellowish or greenish in the case of chlorites, and grayish and brownish in the case of carbonates (Deer *et al.* 1992; Soriano *et al.* 2002). The color and brightness is related to the extent of reflection–diffusion of light on the mineral surface, which is dependent on grain size, grain shape, and roughness of particles, as well as the chemical composition of the mineral powders (Billmeyer & Saltzman 1981; Bundy & Ishley 1991; Bizi *et al.* 2003; Ciullo & Robinson 2003; Gamiz *et al.* 2005).

5. Conclusions

Emirdağ (Afyonkarahisar, Turkey) talc deposit has been formed from alteration of gabbroic rocks of the Mesozoic Yunak ophiolite as lens-shaped pockets and sheet-like bodies in different extensions and directions. This deposit consists of talc, chlorite, actinolite, and a subordinate amount of calcite. Based on semiquantitative results, the Emirdağ samples were classified into 4 groups: i) talc- and chlorite-bearing actinolite (E-1), ii) actinolite-rich talc (E-2), iii) chlorite-bearing talc (E-3), and iv) pure talc (E-4). While the highest amount of talc was observed in the pure talc sample with 95 wt.%, talc mineral was determined as 10 wt.% in talc- and chlorite-bearing actinolite sample. SEM studies revealed that fine-grain, plate, and sheet-like microcrystalline talc crystals are associated with tabular, acicular actinolite, and curved and flake-like chlorite. In places, talc and chlorite are alteration products of actinolites. During alteration of actinolite to talc, Fe and

Table 3. Physicochemical properties of the Emirdağ talc samples.

Physicochemical properties	E-1	E-2	E-3	E-4
Specific surface area, m^2/g	10.85	11.87	11.43	6.65
pH	9.01	9.05	9.53	8.52
Water soluble substance, wt.%	0.13	0.10	0.17	0.11
Acid-soluble iron, wt.%	0.66	0.56	0.59	0.54
Color measurements				
L^*	78.55	86.84	90.82	95.57
a^*	–1.82	–1.76	–0.44	–1.68
b^*	3.17	2.17	7.24	2.54
Whiteness index	76.19	81.96	85.43	89.16

Ca decreased, but conversely Mg and Si increased. EDX analysis of the Emirdağ talc samples was characterized by high SiO_2 (44.35–59.56 wt.%) and MgO (24.08–28.88 wt.%), but low Al_2O_3 (0.49-3.29 wt.%). On the other hand, high Ni (0.21–0.26 wt.%), and Cr (0.20–0.35 wt.%) contents of the Emirdağ samples in chemical analyses are conformable to the composition of talc deposits related to ultramafic origin. Fe_2O_3 content affecting the whiteness of talc varies between 5.40 and 6.10 wt.%. The correlative results obtained from EDX studies conducted on the talc crystals and chemical analyses of the pure talc samples indicated that iron takes place in the crystal lattice structure of talc minerals. Accordingly, high IS (1.26 mm/s) and QS (2.72 mm/s) values obtained from Mössbauer studies also confirm the results of EDX and chemical analysis and indicate that iron in the Emirdağ talc is thought to be Fe^{+2}.

On the other hand, it was observed that the strong peak intensities of the talc on the FT-IR spectra decrease with reduction of the talc content in the samples, and different endothermic/exothermic peaks and mass loss arose in the DTA and TG curves consistently with the mineralogical composition. According to the results of color analysis, the WI and L values increase proportionally with talc content but are inversely proportional to the iron and titanium element contents of the talc samples. Taking into account the physiochemical values, the talc from the Emirdağ region does not have the qualities in its current form, such as high purity, chemical content (particularly Fe_2O_3 and CaO), and other physical properties, especially whiteness, that are required in industries like cosmetics, paint, or paper. However, there might be a possibility of using it as a secondary raw material in these industries.

References

Billmeyer, F.W. & Saltzman, M. 1981. *Principles of Color Technology*. Wiley Interscience, New York.

Bizi, M., Flament, M.P., Baudet, G. & Gayot, A. 2003. Relation between structural characteristics of talc and its properties as an antisticking agent in the production of tablets. *European Journal of Pharmaceutical Sciences* **19**, 373–379.

Brown, G. 1972. *X–Ray Identification and Crystal Structures of Clay Minerals*. Mineral Society, London.

Bundy, W.M. & Ishley, J.N. 1991. Kaolin in paper filling and coating. *Applied Clay Science* **5**, 397–420.

Chung, F.H., 1974. Quantitative interpretation of X-ray diffraction patterns of mixtures. II. Adiabatic principle of X-ray diffraction analysis of mixtures. *Journal of Applied Crystallography*, **7**, 526–531.

Ciullo, P.A. & Robinson, S. 2003. Talc (shape and form meet function). *Paint & Coatings Industry* **19**, 30–34.

Çoban, F. 2004. Mineralogical-geochemical characteristics of Gümeli (İvrindi-Balıkesir) talc occurrences. *Osmangazi Üniversitesi Mühendislik Mimarlık Fakültesi Dergisi*, **17** (in Turkish with English abstract).

Doğan, A.Ü., Doğan, M., Onal, M., Sarikaya, Y., Aburub, A. & Wurster, D.E. 2006. Baseline studies of the Clay Minerals Society source clays: specific surface area by the Brunauer Emmett Teller (BET) method. *Clays and Clay Minerals* **54**, 62–66.

Deer, W.A., Howie, R.A. & Zussman, J. 1992. *An Introduction to the Rock-Forming Minerals*. Longman Scientific & Technical, Essex, UK.

DPT. 2007. *9th Development Plan for 5 Years, The Report of the Special Commission of Mining*. DPT, Ankara (in Turkish).

El-Sharkawy, M.F. 2000. Talc mineralization of ultramafic affinity in the Eastern Desert of Egypt. *Mineralium Deposita* **35**, 346–363.

Farmer, V.C. 1974. The layer silicates. *In:* Farmer, V.C. (ed), *The Infrared Spectra of Minerals*. Mineralogical Society, London, 331–363.

Ferrage, E., Martin, F., Petit, S., Pejo-Soucaille, S., Micoud, P., Fourty, G., Ferret, J., Salvi, S., Parseval, P. & Fotune, J.P. 2003. Evaluation of talc morphology using FT-IR and H/D substitution. *Clay Minerals* **38**, 141–150.

Gamiz, E., Melgosab, M., Sanchez-Maranon, M., Martin M.J.M. & Delgadoa, R. 2005. Relationships between chemico-mineralogical composition and color properties in selected natural and calcined Spanish kaolins. *Applied Clay Science* **28**, 269–282.

Gill, A., Korili, S.A., Trujillano, R.M. & Vicente A. 2011. A review on characterization of pillared clays by specific techniques. *Applied Clay Science* **53**, 97–105.

Gonçalves, M.A., Jesus, F. and Garg, V.K. 1991. Mössbauer study of Brazilian soapstone. *Hyperfine Interactions* **67**, 437–442.

Gören, R., Göçmez, H. & Özgür, C. 2006. Synthesis of cordierite powder from talc, diatomite and alumina. *Ceramic International* **32**, 407–409.

Grim, R.E. 1968. Clay mineralogy, Int. Series in Earth Sciences. McGraw-Hill, New York.

Hiçyılmaz, C., Ulusoy, U. & Yekeler, M. 2004. Effects of the shape properties of talc and quartz particles on the wettability based separation processes. *Applied Surface Science* **233**, 204–212.

Hojamberdiev, M., Kameshima, Y., Nakajima, A., Okada, K. & Kadirova, Z. 2008. Preparation and sorption properties of materials from paper sludge. *Journal of Hazardous Materials* **151**, 710–719.

Hristova, E. & Jancev, S. 2003. Characteristics of calcite limestone-marble from Macedonia used as a flux material. *Journal of Mining and Metallurgy* **39**, 443–451.

Kibici, Y., Yıldız, A., Bağcı, M., & Kavas, T. 2000. Petrography of Büyük Karabağ (Afyon) marbles and their physico-mechanical properties. *Marble* **6**, 92–98 (in Turkish).

Liao, J. & Mamoru, S. 1992. Thermal behavior of mechanically amorphized talc. *Thermochimica Acta* **197**, 295–306.

Lopez-Galindo, A. & Viseras, C. 2004. Pharmaceutical and cosmetic applications of clay. *In:* Wypych, F. & Satyanarayana, K.G. (eds), *Interface Science and Technology: Clay Surfaces* **1**, 267–289.

Marel, H.W. & Beutelspacher, H. 1976. *Atlas of Infrared Spectroscopy of Clay Minerals and their Admixtures*. Elsevier, Amsterdam.

Martin, P.J., Wilson, D.I. & Bonnett, P.E. 2004. Rheological study of a talc-based paste for extrusion-granulation. *Journal of the European Ceramic Society* **24**, 3155–3168.

Metin, S., Genç, S. & Bulut, V. 1987. *Geology of Afyon and Surrounding Regions*. Technical Report. Bulletin of the Mineral Research and Exploration Institute, No: 2113, Ankara (in Turkish).

Moore, D.M. & Reynolds, R.C. 1997. *X-ray Diffraction and the Identification and Analysis of Clay Minerals*. Oxford University Press, Oxford.

MTA. 1980. *The Mine Schedule of Turkey*. Mineral Research and Exploration Institute (MTA), Ankara (in Turkish).

Murad, E. 2006. Mössbauer spectroscopy of clays and clay minerals. *In:* Bergaya, F., Theng, B.K.G. & Lagaly G. (eds), *Handbook of Clay Science: Developments in Clay Science* **1**, 755–764.

Murat, A. & Temur, S. 1995. The talc deposits of Kıraman (Ayrancı-Karaman) district, Turkey. *Geological Bulletin of Turkey* **38**, 95–102 (in Turkish).

Neto, J.B.R. & Moreno, R. 2007. Rheological behaviour of kaolin/talc/alumina suspensions for manufacturing cordierite foams. *Applied Clay Science* **3**, 157–166.

Nkoumbou, C., Njopwouo, D., Villiéras, F., Njoya, A., Yonta Ngouné, C., Ngo Ndjock, L., Tchoua, F.M. & Yvon, J. 2006. Talc indices from Boumnyebel (Central Cameroon), physico-chemical characteristics and geochemistry. *Journal of African Earth Sciences* **45**, 61–73.

Nkoumbou, C., Villieras, F., Njopwouo, D., Ngoune, C., Barres, O., Pelletier, M., Razafitianamaharavo, A. & Yvon, J. 2008a. Physicochemical properties of talc ore from three deposits of Lamal Pougue area (Yaounde Pan-African Belt, Cameroon), in relation to industrial uses. *Applied Clay Science* **41**, 113–132.

Nkoumbou, C., Villieras, F., Barres, O., Bihannic, I., Pelletier, M., Razafitianamaharavo, A., Metang, V., Yonta Ngoune, C., Njopwouo, D. & Yvon, J. 2008b. Physicochemical properties of talc ore from Pout-Kelle and Memel deposits (central Cameroon). *Clay Minerals* **43**, 317–337.

Olabanji, S.O., Ige, A.O., Mazzoli, C., Ceccato, D., Ajayi, E.O.B., De Poli, M. & Moschini, G. 2005. Quantitative elemental analysis of industrial mineral talc, using accelerator-based analytical technique. *Nuclear Instruments and Methods in Physics Research B* **240**, 327–332.

Pérez-Maqueda, L.A., Duran, A. & Pérez-Rodriguez, J.L. 2004. Preparation of submicron talc particles by sonication. *Applied Clay Science* **28**, 245–255.

Prochaska, W. 1989. Geochemistry and genesis of Austrian talc deposits. *Applied Geochemistry* **4**, 511–525.

Rancourt, D.G. 1998. Mössbauer spectroscopy in clay science. *Hyperfine Interactions* **117**, 3–38.

Sanchez-Soto, P.J., Wiewiora, A., Aviles, M.A., Justo, A., Pérez-Maqueda, L.A., Pérez-Rodriguéz, J.L. & Bylina, P. 1997. Talc from Puebla de Lillo, Spain. II. Effect of dry grinding on particle size and shape. *Applied Clay Science* **12**, 297–312.

Schandl, E.S., Sharara, N.A. & Gorton, M.P. 1999. The origin of the Atshan talc deposit in Hamata area, Eastern desert, Egypt: a geochemical and mineralogical study. *The Canadian Mineralogist* **37**, 1211–1227.

Shoval, S. 2003. Using FT-IR spectroscopy for study of calcareous ancient ceramics. *Optical Materials* **24**, 117–122.

Sontevska, V., Jovanovski, G. & Makreski, P. 2007. Minerals from Macedonia. Part XIX. Vibrational spectroscopy as identificational tool for some sheet silicate minerals. *Journal of Molecular Structure* **834**, 318–327.

Soriano, M., Sanchez-Maranon, M., Melgosa, M., Gamiz, E. & Delgado, R. 2002. Influence of chemical and mineralogical composition on colour for commercial talcs. *Color Research and Application* **27**, 430–440.

Speyer, R.F. 1994. *Thermal Analysis of Materials*. Marcel Dekker, New York.

Stuart, B., George, W.O. & Mcintyre, P. 1998. *Modern Infrared Spectroscopy*. John Wiley & Sons, New York.

Taboadela, M.M. & Aleixandre Ferrandis, V. 1957. The mica minerals. *In:* Mackenzie, R.C. (ed), *The Differential Thermal Investigation of Clays*. London Mineralogical Society (Clay Minerals Group), London, 180–181.

Terada, K. & Yonemochi, E. 2004. Physicochemical properties and surface free energy of ground talc. *Solid State Ionics* **172**, 459–462.

Thorez, J. 1976. *Practical Identification of Clay Minerals*. G. Lelotte, Dison, Belgium.

Tomaino, G.P. 2000. Talc and pyrophyllite. *Mining Engineering* **57**, 64–65.

TS EN ISO 3262-10, March 2002. *Filling materials for paints (Properties and experimental methods)*. Turkish Standard Institute, Ankara (in Turkish).

TS 2973, February 1978. *Talc-used in cosmetics industry*. Turkish Standard Institute, Ankara (in Turkish).

TS 10521, December 1992. *Talc-used in paper industry*. Turkish Standard Institute, Ankara (in Turkish).

Turhan, N. 2002. *Geology Maps of Turkey, Section of Ankara*. General Directorate of Mineral Research and Exploration, Ankara (in Turkish).

Ulusoy, U. 2008. Application of ANOVA to image analysis results of talc particles produced by different milling. *Powder Technology* **188**, 133–138.

Van Der Marel, H.W. & Beutelspacher, H., 1976. *Atlas Of Infrared Spectroscopy of Clay Minerals and Their Admixtures*. Elsevier, Amsterdam.

Van Olphen, H. 1977. *Clay Colloid Chemistry (second edition).* John Wiley & Sons, New York.

Wallqvist, V., Claesson, P.M., Swerin, A., Schoelkopf, J. & Gane, P.A.C. 2009. Influence of wetting and dispersing agents on the Interaction between talc and hydrophobic particles. *Langmuir* **25**, 6909–6915.

Wang, J. & Somasundaran, P. 2005. Absorption and conformation of carboxymethylcellulose at solid-liquid interfaces using spectroscopic, AFM and allied techniques. *Journal of Colloid and Interface Science* **291**, 75–83.

Wilkins, R.W.T. & Ito, J. 1967. Infrared spectra of some synthetic talcs. *American Mineralogist* **52**, 1649–1661.

Wilson, M.J. 1995. *Clay Mineralogy: Spectroscopic and Chemical Determinative Methods*. Chapman & Hall, New York, 52–55.

Xie, A.J., Zhang, C.Y., Shen, Y.H., Qiu, L.G., Xiao, P.P. & Hu, Z.Y. 2006. Morphologies of calcium carbonate crystallites grown from aqueous solutions containing polyethylene glycol. *Crystal Research Technology* **41**, 967–971.

Yalçın, H. & Bozkaya, Ö. 2006. Mineralogy and geochemistry of Paleocene ultramafic- and sedimentary-hosted talc deposits in the southern part of the Sivas basin, Turkey. *Clays and Clay Minerals* **54**, 333–350.

Yang, H., Du, C., Jin, S. & Tang, A. 2007. Preparation and characterization of SnO_2 nanoparticles incorporated into talc porous materials (TPM). *Material Letters* **61**, 3736–3739.

Yuan, J. & Murray, H.H. 1997. The importance of crystal morphology on the viscosity of concentrated suspensions of kaolins. *Applied Clay Science* **12**, 209–219.